

# Equation for the Density of Particle-Reinforced Metal Matrix Composites: A New Approach

S.C. Sharma

(Submitted 27 December 2002; in revised form 21 January 2003)

This paper presents a novel equation for the density of ceramic particle reinforced metal matrix composites. An overall density change occurs in composites due to the thermal mismatch between the metal matrix and the reinforcement. The thermal mismatch occurs because the coefficient of thermal expansion and the elastic properties are different for the matrix and the reinforcement. The values obtained using the proposed equation for density were compared with both the rule of mixtures for density and the experimental values obtained for aluminium and zinc alloy composites. The composite specimens were fabricated using compositing technique (one of the types of liquid metallurgy route). The proposed mathematical model is found to have better agreement with the experimental results at lower volume fractions of the reinforcement; however, some deviations were observed at higher volume fractions of the reinforcement. The proposed equation yields agreeable results for aluminium composites and fairly agreeable results for zinc alloy composites.

**Keywords** composites, density, proposed model, rule of mixtures

## 1. Introduction

The demand for high strength and stiffness and low-density materials has given considerable importance to the manufacturing aspects of particle reinforced metal matrix composites (MMCs). MMCs are potential materials for technological applications because they exhibit higher stiffness,<sup>[1]</sup> lower thermal expansion,<sup>[2]</sup> lower thermal conductivity,<sup>[3]</sup> better damping properties,<sup>[4]</sup> and higher wear resistance<sup>[5]</sup> than conventional alloys. MMCs are increasingly used in many engineering applications, in products such as automobile parts (i.e., piston liners, clutches, pulleys, etc.), aircraft components, sports goods, etc.<sup>[6]</sup>

As the composite materials are being increasingly considered for specific application, many researchers have studied MMCs by different methods, such as shear-lag theory for elastic constants,<sup>[7]</sup> finite element analysis for mechanical properties,<sup>[8,9]</sup> boundary element analysis,<sup>[10]</sup> mean-field theory,<sup>[11]</sup> and rule of mixtures. Several theories like the ones mentioned above have been proposed for explaining the various properties of the MMCs. The physical, mechanical, chemical, and electrical properties of MMCs are influenced by the thermomechanical properties of the matrix and the reinforcement. Some researchers have also studied the effect of the coefficient of thermal expansion (CTE) on the mechanical properties of the composites.<sup>[12-14]</sup>

The existing rule of mixtures law for the density of the MMCs, does not consider the mismatch in the CTE, and the

elastic constants between the matrix and the reinforcement, which affect the density of the composites. Trojanova et al. have pointed out that when MMCs are cooled, misfit strains might set in if large differences exist between the thermal expansion coefficients of the matrix and the reinforcement.<sup>[15]</sup> This strain induces thermal stresses that may create dislocations and lead to an increase in the dislocation density. Budiansky et al. neglected any shear effect and considered the case in which the reinforced particles were allowed to undergo only a volumetric strain, which leads to a higher density of matrix alloy around the particles.<sup>[16]</sup> Some authors have also pointed out the presence of the dislocation density of the matrix alloy around the particles using traveling electron microscopy.<sup>[17-20]</sup>

In the present work, an attempt has been made to analyze the effect of thermomechanical properties (CTE and elastic constants) on the density of the MMCs. The objective is to present an analytical model to predict the density of MMCs and compare the values obtained by the proposed model both with the rule of mixtures law and the experimental values obtained for aluminium and zinc alloy composites fabricated by compositing.

## 2. Theoretical Analysis

The rule of mixtures for the density of MMCs considers only the densities of the matrix and the reinforcement represented by the two concentric circles, as shown in the Fig. 1(a), disregarding their CTE and elastic properties, leading to inaccurate density predictions. Hence, the rule of mixtures holds good only when the CTE and the elastic properties of the matrix and the reinforcement are the same. Practically, both the CTE and the Poisson's ratio of the ceramic particle reinforcement are much lower than that of any metal matrix. The matrix tries to shrink more than that of the reinforcement during cooling, which is actually hindered by the reinforcement, which induces volumetric strain in the matrix as well as the reinforcement. The conceptual understanding of this is shown in

S.C. Sharma, Professor and Head Research and Development, Department of Mechanical Engineering, R.V. College of Engineering, Bangalore-560 059, Karnataka, India. Contact e-mail: rvrds@blr.vsnl.net.in.

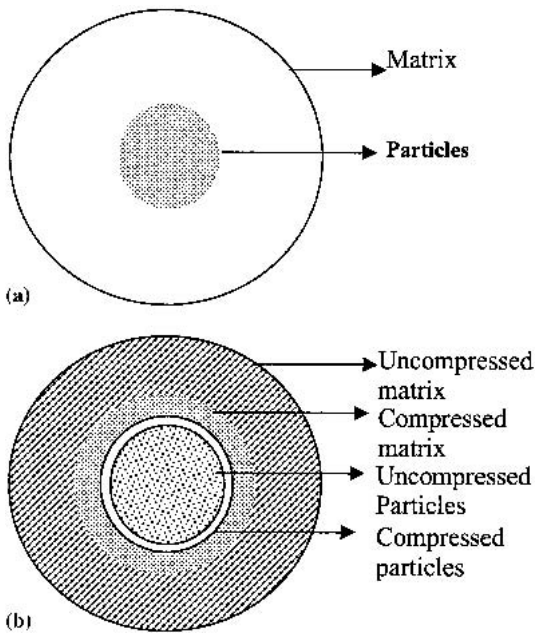


**Fig. 1** (a) Two concentric circles representing the density of the matrix and the reinforcement without considering thermal mismatch and (b) four concentric circles representing the density of uncompressed matrix, compressed matrix, uncompressed particulate, and compressed particulate

Fig. 1(b) as four concentric spheres, namely uncompressed matrix, compressed matrix, uncompressed reinforcement, and compressed reinforcement. The thickness of the layers corresponding to the four concentric spheres depends upon the CTE and the elastic constants of the reinforcement and the matrix.

The analytical approach is based on the following assumptions (they are similar to those used for the analysis of elastic problems<sup>[21-24]</sup>):

- 1) The particles are spheres of uniform radius.
- 2) No void exists in the composite.
- 3) The matrix and the reinforcement particle exhibit perfectly elastic behavior.
- 4) The temperature in the MMCs is uniform in all directions (no thermal gradient).
- 5) The stress-strain behavior is independent of the strain rate and the stress orientation.

The proposed model estimates density considering CTE and elastic properties of both the matrix and the reinforcement. At their melting temperatures, the metal and the reinforcement are in stress free state. During solidification, the matrix metal tries to shrink more than that of the ceramic particulate. Due to this misfit shrink, volumetric strain occurs at the interface of the particle and the matrix, as shown in Fig. 2.

The total mass of the composite  $m_c$  is the sum of the masses of the matrix  $m_m$  and the reinforcement  $m_r$ <sup>[24]</sup>:

$$\text{i.e., } m_c = m_r + m_m \quad (\text{Eq 1})$$

The volume of composite  $v_c$ , however, should include the volume of voids  $v_v$  and the volume shrinkage due to thermal mismatch  $\delta v_{sh}$ . Thus,

$$v_c = v_r + v_m + v_v - \delta v_{sh}, \quad (\text{Eq 2})$$

where  $v_m$ ,  $v_r$ , and  $v_v$  represent the volumes of the matrix, reinforcement, and voids, respectively.

In the absence of voids (as assumed above),

$$v_c = v_r + v_m - \delta v_{sh} \quad (\text{Eq 3})$$

The composite density  $\rho_c$  is then given by

$$\rho_c = \frac{m_c}{v_c} = \frac{(m_r + m_m)}{(v_r + v_m - \delta v_{sh})} \quad (\text{Eq 4})$$

$\delta v_{sh}$  can be resolved into two components, i.e., volume shrinkages of the matrix ( $\delta v_{shm}$ ) and the particulate ( $\delta v_{shr}$ ):

$$\delta v_{sh} = \delta v_{shm} + \delta v_{shr} \quad (\text{Eq 5})$$

The above equation can be rewritten as (by multiplying and dividing by their volumes)

$$\delta v_{sh} = \frac{\delta v_{shm} \times v_m}{v_m} + \frac{\delta v_{shr} \times v_r}{v_r} \quad (\text{Eq 6})$$

Substituting (volumetric strain,  $\varepsilon = \delta v/v$ ),

$$\delta v_{sh} = \varepsilon_m v_m + \varepsilon_r v_r \quad (\text{Eq 7})$$

where  $\varepsilon_m$  and  $\varepsilon_r$  are the volumetric strains of the matrix and the particulate, respectively. Assuming that the size of particulate is very small and is spherical in shape  $\varepsilon$  can be written as

$$\varepsilon = \frac{\sigma_r}{B} \quad (\text{Eq 8})$$

where  $\sigma_r$  is the radial stress, which occurs at the interface between the particle and the matrix due to the thermal mismatch and  $B$  is the Bulk modulus. The Eq 7 can be rewritten as

$$\delta v_{sh} = \frac{\sigma_{rm} v_m}{B_m} + \frac{\sigma_{rr} v_r}{B_r} \quad (\text{Eq 9})$$

where  $B_m$  and  $B_r$  are the bulk moduli of the matrix and the reinforcement, and  $\sigma_{rm}$  and  $\sigma_{rr}$  the radial stress of the matrix and the reinforcement.

The elastic stress ( $\sigma_r$ ) components at the interface between the matrix and reinforcement are equal and opposite to each other, i.e.,

$$\sigma_{rm} = \sigma_{rr} = \sigma_r \quad (\text{Eq 10})$$

Substituting Eq 10 into Eq 9,

$$\delta v_{sh} = \sigma_r \left( \frac{v_m}{B_m} + \frac{v_r}{B_r} \right) \quad (\text{Eq 11})$$

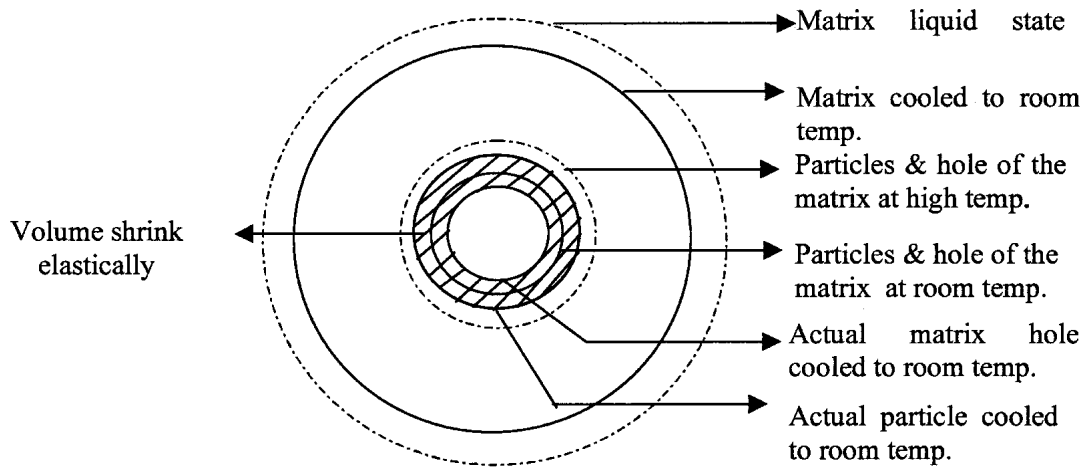


**Fig. 2** Volume shrinkage due to the thermal mismatch (difference in the CTE between the particle and the matrix metal) during cooling of the molten metal

The general relation between the elastic modulus and the bulk modulus is

$$B = \frac{E}{3(1 - 2\nu)} \quad (\text{Eq 12})$$

where  $E$  and  $\nu$  are the Young's modulus and Poisson's ratio, respectively.

Substituting Eq 12 into Eq 11,

$$\delta v_{sh} = 2\sigma_r \left( \frac{\nu_m 3(1 - 2\nu_m)}{E_m} + \frac{\nu_r 3(1 - 2\nu_r)}{E_r} \right) \quad (\text{Eq 13})$$

where  $E_m$  and  $E_r$  are the Young's moduli of the matrix and the reinforcement and  $\nu_m$  and  $\nu_r$  are Poisson's ratio of the matrix and the reinforcement.

Substituting Eq 13 into Eq 4, we get

$$\rho_c = \frac{(m_r + m_m)}{\nu_r + \nu_m - 2\sigma_r \left( \frac{\nu_m 3(1 - 2\nu_m)}{E_m} + \frac{\nu_r 3(1 - 2\nu_r)}{E_r} \right)} \quad (\text{Eq 14})$$

The thermal residual stress ( $\sigma_r$ ) occurs due to the mismatch between the CTE of the two phases (matrix and reinforcement), the magnitude of the thermal decrement (from cooling), and the relative values of the elastic constant of both the reinforcement and the matrix metal.

The mismatch stresses within the matrix can be calculated using the Hooke's law, in terms of the elastic strain and the stiffness tensor of the material ( $E_m$ )

$$\sigma_r = E_m (\varepsilon^c - \varepsilon^T) \quad (\text{Eq 15})$$

where  $\varepsilon^c$  is the constrained strain and  $\varepsilon^T$ , the specific shape change.

According to Eshelby<sup>[25]</sup>

$$\varepsilon^c = S \varepsilon^T \quad (\text{Eq 16})$$

$S$  is the Eshelby tensor, which can be calculated in terms of the reinforcement aspect ratio and Poisson's ratio of the material.

Substituting Eq 16 into Eq 15,

$$\sigma_r = E_m (S - I) \varepsilon^T \quad (\text{Eq 17})$$

where  $I$  is the identity matrix.

Considering the mismatch strain between reinforcement and matrix,

$$\sigma_r = E_r (\varepsilon^c - \varepsilon^{T*}) \quad (\text{Eq 18})$$

where  $\varepsilon^{T*} = (\alpha_m - \alpha_r) \Delta T$  (thermal strain),  $\alpha_m$ ,  $\alpha_r$ , and  $\Delta T$  are the CTE of the matrix, CTE of the reinforcement, and temperature gradient, respectively.

The internal stresses in the equivalent reinforcement must be identical. Therefore equating the right hand side of Eq 15 and 18,

$$E_r (\varepsilon^T - \varepsilon^{T*}) = E_m (S - I) \varepsilon^T \quad (\text{Eq 19})$$

Rearranging the terms,

$$\varepsilon^T = [(E_r - E_m) S + E_m]^{-1} E_r \varepsilon^{T*} \quad (\text{Eq 20})$$

Substituting Eq 20 into Eq 17,

$$\sigma_r = E_m E_r (S - I) (\alpha_m - \alpha_r) \Delta T / [(E_r - E_m) S + E_m]^{-1} \quad (\text{Eq 21})$$

Hence, substituting Eq 21 into Eq 14, we get the equation for density of an MMC

**Table 1 Physical Properties of the Ceramic and the Metal Alloys**

Materials	Chemical Composition	Density, g/cm <sup>2</sup>	Young's Modulus, GPa	Poisson's Ratio	CTE 10 <sup>-6</sup> /°C
Albite	SiO <sub>2</sub> Al <sub>2</sub> O <sub>3</sub> Na <sub>2</sub> O <sub>3</sub>	2.6	75	0.27	2.03
Garnet	Ca <sub>2</sub> Fe <sub>2</sub> (SiO <sub>4</sub> ) <sub>3</sub>	3.1	80	0.14	2.05
Quartz	SiO <sub>2</sub>	2.65	96	0.27	1.37
Zircon	ZrO <sub>2</sub> SiO <sub>2</sub>	4.5	220	0.26	2.02
Al6061	Mg-0.92, Si-0.76, Ti-0.1, Zn-0.06, Be-0.003, Fe-0.28, Cu-0.22, Cr-0.07, Mn-0.04, v-0.01, Al-Balance, all in wt.%	2.7(a)	70	0.3	22.8
ZA-27	Al-25-28, Mg-0.01-0.02, Cu-2-2.5, Zinc-Balance, all in wt.%	2.615(b) 5.1(a) 5.05(b)	76	0.3	36

(a) Standard data handbook

(b) Measured density value

CTE, coefficient of thermal expansion

$$\rho_c = \frac{(m_r + m_m)}{v_r + v_m - 2 E_m E_r (S - I) (\alpha_m - \alpha_r)} \Delta T / [(E_r - E_m) S + E_m]^{-1} \left( \frac{v_m 3 (1 - 2 v_m)}{E_m} + \frac{v_r 3 (1 - 2 v_r)}{E_r} \right) \quad (\text{Eq 22})$$

### 3. Experimental Procedure

#### 3.1 Materials Selection

Al 6061 and ZA-27 alloys are used as matrix metal alloys. Albite (grey in color), garnet (brown in color), and zircon (yellow in color) are naturally occurring plagioclase feldspar. Basically consisting of silicates (R-SiO<sub>2</sub>), they are abundantly available in the earth's crust. Quartz (milky white in color) is natural silicon oxide. These ceramics are as used as reinforcements. The chemical compositions and properties of matrix metal alloys and reinforcements are presented in Table 1.

#### 3.2 Composite Preparation

Albite/Al 6061, garnet/Al 6061, zircon/ZA 27, and quartz/ZA 27 composites were considered for the study. The compo-casting technique was used to prepare the composite specimens.<sup>[26]</sup> In this process, the matrix alloy was first superheated above its melting temperature, and stirring was initiated to homogenize the temperature. The temperature was then lowered gradually until the alloy reached a semi-solid state. At this temperature, the preheated ceramic particles of nominal size of 30-50 mm were introduced into the molten slurry. The melt was then superheated above its liquidus temperature and finally poured into the lower die-half of the press, and the top die was brought down to solidify the composite by applying high pressure of 25 MPa.

#### 3.3 Volume Fraction Determination

Volume fraction of MMCs was determined using disintegrated melt deposition process (chemical dissolution method).<sup>[27]</sup> The weighed specimens were completely immersed in 1 N hydrochloric acid to dissolve the metal alloy and

then filtered to separate the reinforcement particulate. The particulates were then dried and weighed to determine the volume fraction of the MMCs using

$$\text{Volume fraction} = \frac{\text{Final weight of the reinforcement} \times \text{density of matrix}}{\text{Initial weight of the composite} \times \text{density of reinforcement}}$$

#### 3.4 Density Measurement

Machined and polished composite specimens (10 mm diameter and 5 mm length, sample size 4) were considered for density measurement using the Archimedian method at room temperature (27 °C and relative humidity of 48%). The beaker with water was initially kept on the electronic balance (accuracy 0.1 mg) set to read zero. The initially weighed, freely suspended specimen (say, W1 mg) was fully immersed in the beaker. The final weight (W2 mg) shown by the balance represents the volume of the displaced water (specific gravity of water = 1) is equivalent to the volume of the specimen. The ratio of W1 to W2 represents the density of the specimen.

## 4. Results and Discussion

#### 4.1 Experimental Results

Figures 3 and 4 depict the density values obtained by (1) rule of mixtures, (2) experimental results, and (3) proposed model, for Al and ZA27 MMCs, respectively.

Figure 3(a) shows the density values of garnet/Al 6061 MMCs. The density of the composite increases with the volume fraction of the reinforcement due to the higher density of garnet particulate.

Figure 3(b) shows the density values of albite/Al6061 MMCs. The density of the composite marginally decreases with increase in volume fraction of the reinforcement due to the lower density of the albite particulate.

Figure 4(a) and (b) show the density of quartz/ZA27 and zircon/ZA27 MMCs. The density of the composite in both the

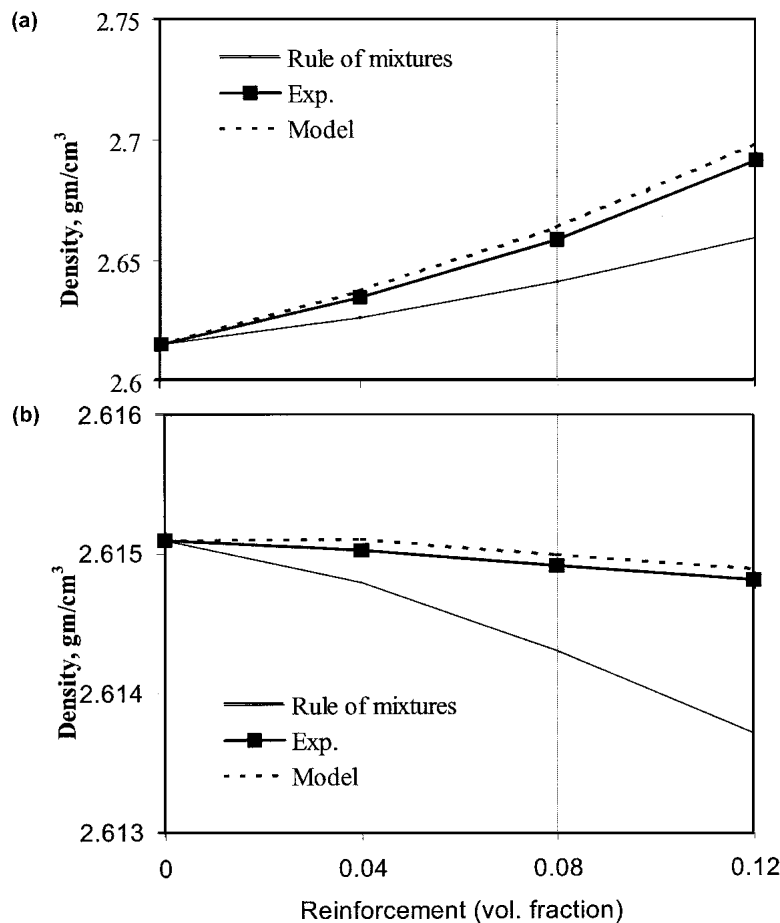


**Fig. 3** Comparison of the density (a) of an Al6061-garnet reinforced composite and (b) of an Al6061-albite reinforced composite

cases decreases with increase in the volume fraction of the reinforcement, due to the lower density of the reinforcement.

#### 4.2 Comparison of Experimental Values With Rule of Mixtures and the Proposed Model

In Al6061/albite and Al6061/garnet MMCs, the experimental values of density show good agreement with that calculated from the developed model. The experimental values are between the values derived from the proposed model and the rule of mixtures. The density values obtained by using the newly developed model are in good agreement with that of experimental values for lower volume fractions, whereas some deviation is observed at higher volume fractions. In particulate-reinforced composites, increasing the reinforcement volume could also result in an increase in the porosity of the MMCs due to the decrease in the inter-particle spacing.<sup>[28]</sup> Surface and interface-porosity of the composites tend to decrease the density of the MMCs. This might cause the deviation in the predicted density values at higher volume fractions of the reinforcement.

The densities of ZA27/quartz and ZA-27/zircon calculated using the model are in agreement with the experimental results but for small deviation. It may be due to the size of ceramic particle, which exceeds the critical size as the crack extension

occurs along the brittle-matrix particle interface upon cooling. Residual stresses generated during cooling to room temperature can also cause crack extension at the brittle matrix/particle interface.<sup>[28-31]</sup> Some authors have investigated the stress distributions created around and within hard particles, which leads to the cracks in both the reinforcement and the matrix.<sup>[32]</sup> As a result, radial cracks appear in the interfacial region along the whole circumference of the interface.<sup>[33]</sup> Smith et al. have observed radial cracking in the interfacial region of the MMCs.<sup>[34]</sup> Under this condition, the model predicts higher density values than the experimental values.

#### 4.3 Accuracy of the Proposed Model

The densities of the MMCs of different alloy compositions have been evaluated using a proposed model and compared with the experimental values. The percentage deviations have been computed as shown in Table 2. It is evident from the tabulated values that the percent of deviation varies from 0.003 to 0.139, which demonstrates the accuracy of the model.

### 5. Conclusion

In the present investigation, an equation was derived for the density of the MMCs taking into consideration the thermome-

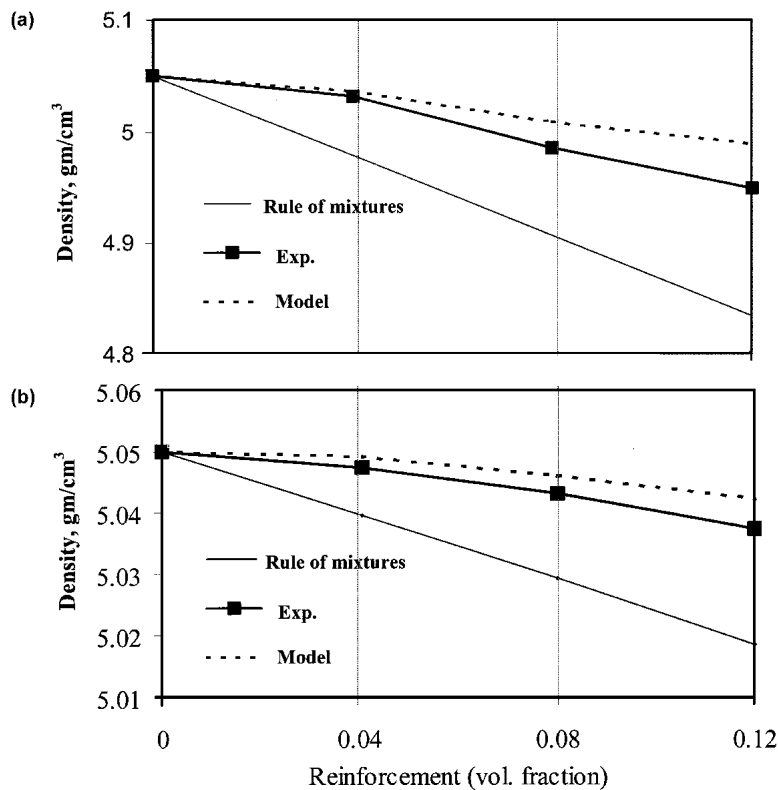


Fig. 4 Comparison of the density (a) of a ZA27-quartz reinforced composite and (b) of a ZA27-zircon reinforced composite

Table 2 Accuracy of the Proposed Model

Material	Volume Fraction	Density Values Obtained		
		By Experiment	Using the Proposed Model	Deviation, %
Al/garnet composites	0.04	2.6341	2.6343	0.011
	0.08	2.6581	2.6586	0.019
	0.12	2.6907	2.6913	0.023
Al/albite composites	0.04	2.6150	2.6151	0.003
	0.08	2.6149	2.6150	0.004
	0.12	2.6148	2.6149	0.004
ZA-27/quartz composites	0.04	5.0470	5.0490	0.040
	0.08	5.0355	5.0400	0.090
	0.12	5.0190	5.0240	0.139
ZA-27/zircon composites	0.04	5.0474	5.0491	0.030
	0.08	5.0430	5.0459	0.060
	0.12	5.0373	5.0423	0.100

chanical properties of both the matrix and the reinforcement. The results were compared with the rule of mixtures for density and experimental values. Based on this study, the following conclusions are arrived at:

- 1) The developed model shows good agreement with experimental density values.
- 2) The model predicts density better than the rule of mixtures.
- 3) In brittle-matrix composites, the experimental values slightly deviated away from the proposed model.

## References

1. S.C. Sharma, B.M. Girish, B.M. Satish, and R. Kamath: *JMEP*, 1998, 7(1), p. 93.
2. S.C. Sharma: *Metall. Trans.*, 2000, 31A, p. 773.
3. L. Keith, R. Karasek, and L. Berk: *J. Appl. Phys.*, 1981, 53(3), p. 1370.
4. J.E. Bishop and V.K. Kinra: *Metall. Trans. A*, 1995, 26A, p. 2773.
5. S.C. Sharma, B.M. Girish, R. Kamath, and B.M. Satish: *Wear*, 1997, 213, p. 33.
6. H.A. Hanna and F. Shehata: *Inst. Lubrication Eng.*, 1993, 49(6), p. 473.
7. V.C. Nardone and K.M. Prewo: *Scripta Metall.*, 1986, 20, pp. 43-50.
8. H. Hung and M.B. Bush: *Mater. Sci. Eng.*, 1997, A232, p. 63.
9. H. Tota, T. Gouda, and M. Kobayashi: *Mater. Sci. Eng.*, 1998, 14, p. 925.
10. M.B. Bush: *Mater. Sci. Eng.*, 1992, A154, p. 139.
11. O.B. Pederson: *Acta Metall.*, 1983, 31, p. 139.
12. M. Hoffman, S. Skirl, W. Pompe, and J. Rodel: *Acta Mater.*, 1999, 47, p. 565.
13. E.U. Lee: *Metall. Trans. A*, 1992, 23A, p. 2205.
14. Y.T. Ziu and J.H. Devletian: *Metall. Trans. A*, 1992, 23A, p. 451.
15. Z. Trojanova, M. Pahutova, J. Kiehn, P. Lukac, and K.U. Kainer: *in Proceedings of the 1st International Conference, San Sebastian, Spain*, Sept 1996, p. 1001.
16. B. Budiansky, J.W. Hutchinson, and J.C. Lambropoulos: *Int. J. Solids Struct.*, 1983, 19, p. 337.
17. M. Vogelsang, R.J. Arsenault, and R.M. Fisher: *Metall. Trans.*, 1986, 17A, p. 379.
18. R.J. Arsenault and N. Shi: *Mater. Sci. Eng.*, 1986, 81, p. 175.
19. R.J. Arsenault, L. Wang, and C.R. Feng: *Acta Metall. Mater.*, 1991, 39, p. 47.
20. N. Shi, B. Wilner, and R.J. Arsenault: *Acta Metall. Mater.*, 1992 40, p. 2841.
21. H.H. Ledbetter and M.W. Ausin: *Mater. Sci. Eng.*, 1989, 89, p. 53.
22. R. Hill: *The Mathematical Theory of Plasticity*, Oxford University Press, London, U.K., 1950, p. 97.

23. D.C. Dunand and A. Mortensen: *Acta Metall.*, 1991, 39, p. 127.
24. K.K. Chawla: *Composite Materials*, Springer-Verlag, New York, 1987, p. 177.
25. J.D. Eshelby: "Elastic Inclusions and Inhomogeneities" in *Progress in Solid Mechanics* 2, I.N. Sneddon and R. Hill, ed., North-Holland, Amsterdam, The Netherlands, 1961, pp. 89-140.
26. R. Meharabian, R.G. Fick, and M.C. Flemings: *Metall. Trans. A*, 1974, 5, p. 1899.
27. M. Gupta, T.S. Srivastan, F.A. Mohamed, and E.J. Lavernia: *J. Mater. Sci.*, 28, 1993, p. 2245.
28. Y.M. Ito, M. Rosenblatt, L.Y. Cheng, F.F. Lange, and A.G. Evans: *Inst. J. Fract.*, 1981, 17, p. 483.
29. F.F. Lange: *Fracture Mechanics of Ceramics*, 1974, 2, p. 599.
30. C.K. Chao and L.Y. Kuo: *J. Thermal Stresses*, 1994, 17, p. 271.
31. X.Q. Xu and D.F. Watt: *Acta Mater.*, 44, 1996, p. 801.
32. D.F. Watt, X.Q. Xu, and D.J. Lloyd: *Acta Mater.*, 1996, 44, p. 789.
33. L.L. Shaw and D.B. Miracle: *Acta Mater.*, 1996, 44(5), p. 2043.
34. P.R. Smith, C.G. Rhodes, and W.C. Revelos: *Interfaces in Metal-Ceramics Composites*, The Minerals, Metals and Materials Society, Warrendale, PA, 1989, p. 35.